CORE
Metadata, citation and similar papers at core.ac.uk
Provided by Elsevier - Publisher Connector
Immunity, Vol. 21, 561–574, October, 2004, Copyright ©2004 by Cell Press

Dyslipidemia Associated with Atherosclerotic Disease Systemically Alters Dendritic Cell Mobilization

Véronique Angeli,[1] Jaime Llodrá,[1] James X. Rong,[2] Kei Satoh,[3] Satoshi Ishii,[4] Takao Shimizu,[4] Edward A. Fisher,[2] and Gwendalyn J. Randolph[1,]*
[1]Department of Gene and Cell Medicine
Mount Sinai School of Medicine
New York, New York, 10029
[2]The Marc and Ruti Bell Vascular Biology and Disease Program and
The New York University Lipid Treatment and Research Center
New York University
New York, New York 10016
[3]Department of Vascular Biology
Hirosaki University School of Medicine
Hirosaki 036-8562
Japan
[4]Department of Biochemistry and Molecular Biology
Faculty of Medicine
University of Tokyo
Tokyo 113-0033
Japan

Summary

High LDL and/or low HDL are risk factors for atherosclerosis and are also a common clinical feature in systemic lupus erythematosus, rheumatoid arthritis, and psoriasis. Here, we show that changes in lipid profiles that reflect atherosclerotic disease led to activation of skin murine dendritic cells (DCs) locally, promoted dermal inflammation, and induced lymph node hypertrophy. Paradoxically, DC migration to lymph nodes was impaired, suppressing immunologic priming. Impaired migration resulted from inhibitory signals generated by platelet-activating factor (PAF) or oxidized LDL that acts as a PAF mimetic. Normal DC migration and priming was restored by HDL or HDL-associated PAF acetylhydrolase (PAFAH), which mediates inactivation of PAF and oxidized LDL. Thus, atherosclerotic changes can sequester activated DCs in the periphery where they may aggravate local inflammation even as they poorly carry out functions that require their migration to lymph nodes. In this context, HDL and PAFAH maintain a normally functional DC compartment.

Introduction

Atherosclerosis is a chronic inflammatory disease of the arterial vasculature (Libby, 2002), and the possibility that atherosclerosis is an autoimmune disease has been discussed (Palinski and Witztum, 2000; Wick et al., 2004). Early lesions of atherosclerosis result from the subendothelial accumulation of low-density lipoprotein (LDL) that when trapped in the vessel wall undergoes modifications, particularly oxidation. Oxidized LDL triggers the production of proinflammatory cytokines and chemokines that induce the recruitment of monocytes (Ross, 1993). Uptake of these modified lipoproteins by differentiating monocytes leads to the formation of the lesions.

Oxidation of LDL also generates a variety of immunogenic epitopes, formed either by oxidized lipids or by adducts between oxidation products and associated proteins. These neoepitopes elicit autoimmune responses as demonstrated by the detection of autoantibodies reacting with oxidized LDL, but not native LDL, in plasma (Orekhov et al., 1991; Palinski et al., 1994). Oxidation of phosphatidylcholine in LDL generates molecules that structurally resemble the inflammatory mediator platelet-activating factor (PAF) (McIntyre et al., 1999) and even bind to PAF receptor (Heery et al., 1995; Marathe et al., 1999). These oxidized metabolites are recognized by an innate B1 cell-derived IgM that normally binds to the PAF-like moiety in *Streptococcus pneumoniae* (Binder et al., 2003; Briles et al., 1982), suggesting that humoral recognition of oxidized LDL occurs through molecular mimicry. Amplification of the titers of this antibody decreases the progression of atherosclerosis by neutralizing and possibly promoting the clearance of oxidized LDL, instead of being pathogenic (Binder et al., 2003; Palinski et al., 1995).

Autoantibodies recognizing oxidized LDL are not only found in atherosclerosis but also in several autoimmune disorders like systemic lupus erythematosus (SLE), psoriasis, and rheumatoid arthritis (RA) (Amara et al., 1995; Cvetkovic et al., 2002; Hayem et al., 2001; Orem et al., 1999; Wu et al., 1999). Elevated titers of these antibodies in SLE, psoriasis, and RA coincides with increased levels of very low-density lipoprotein, LDL, or oxidized LDL and correspondingly decreased levels of high-density lipoprotein (HDL) and apolipoprotein A-I (ApoA-I), the major apoprotein in HDL (Burger and Dayer, 2002; Ilowite et al., 1988; Tselepis et al., 1999). Despite clinical data linking dyslipidemia to autoimmune disorders, basic research to address how dyslipidemia itself may affect the immune system has just recently begun to receive attention (Aprahamian et al., 2004).

Here, we explored how dendritic cell (DC) function is affected by dyslipidemia that occurs in mice lacking apolipoprotein E (ApoE) or LDL receptor. We probed DC functions in the skin and draining lymph nodes (LNs), since the skin is a major target organ in many autoimmune diseases. The study reveals an initial period of spontaneous activation of skin DCs during early weeks of dyslipidemia, followed by a subsequent strong depression of mobilization to LNs, which leads, at this stage, to poor immunologic priming. We further uncover a critical role for HDL and its associated enzyme PAF acetylhydrolase (PAFAH) in maintaining normal DC migration and immunization.

Results

Systemic Age-Dependent and Diet-Accelerated Hypertrophy of LNs in *Apoe*$^{-/-}$ Mice

A diet rich in fat and cholesterol (Western diet) accelerates disease in *Apoe*$^{-/-}$mice, but the strain develops

*Correspondence: gwendalyn.randolph@mssm.edu

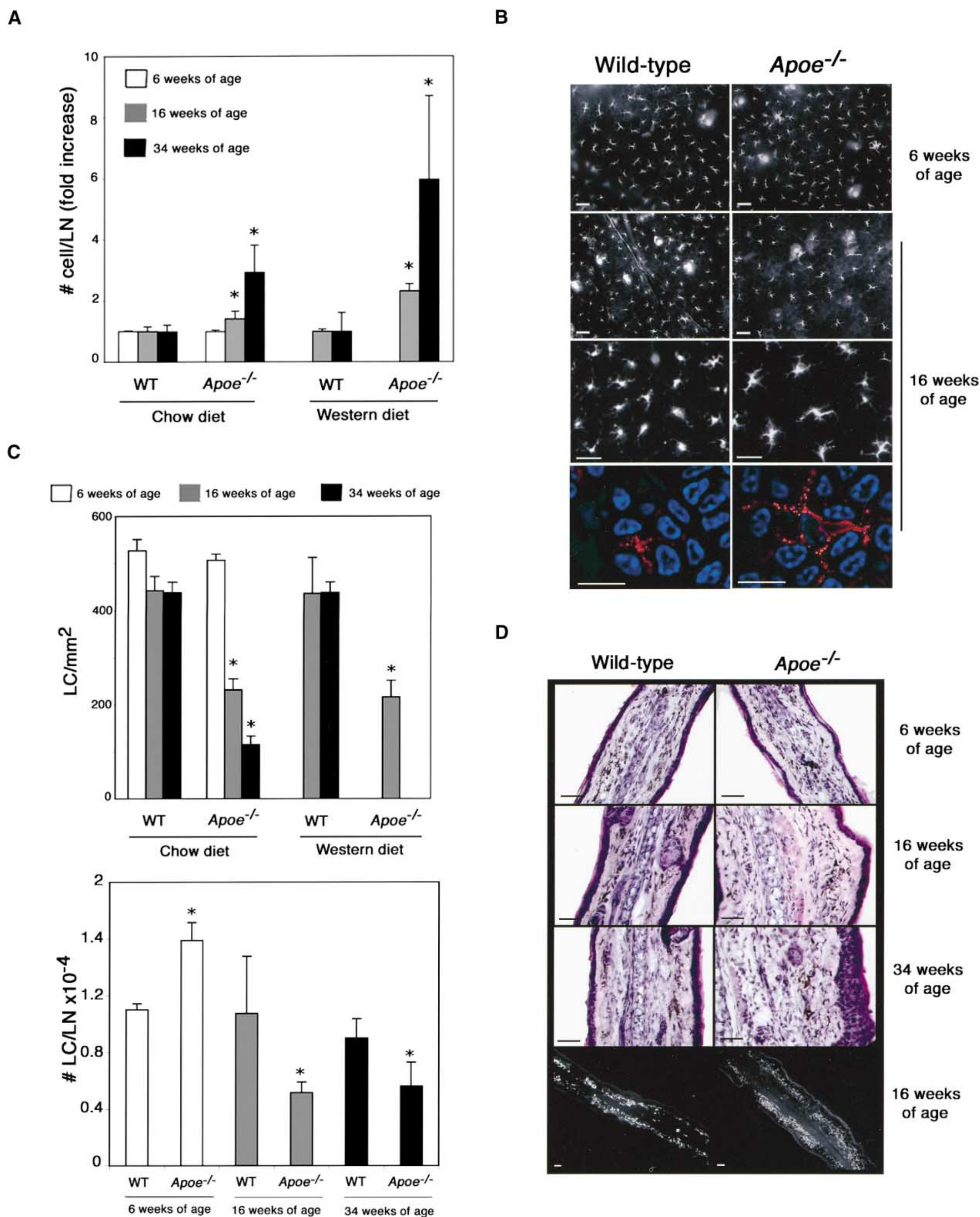

Figure 1. Perturbations in LNs and Skin of *Apoe*$^{-/-}$ Mice

Wt and *Apoe*$^{-/-}$ mice were studied at 6, 16, and 34 weeks of age. Some were placed on a Western diet at 6 week of age.

(A) Relative number of cells in skin-draining LNs was determined in order to combine values from the four experiments conducted (n = 4). By 16 weeks and thereafter, the values between wt and atherosclerotic mice were significantly different; $p < 0.05$ independent of diet type.

(B) Epidermal sheets from wt and *Apoe*$^{-/-}$ mice were stained with anti-IA^b mAb. Low power (top two rows) and high power (last two rows) magnifications are shown. For analysis of MHC class II distribution, epidermal sheets were stained with anti-IA^b mAb (red) and DAPI (blue).

(C) The number of LC/mm^2 was evaluated (upper panel). Values between wt and atherosclerotic mice were significantly different, $p < 1 \times 10^{-5}$. The number of LCs per LN was calculated by multiplying the percentage of langerin-positive cells by the number of total LN cells (bottom). Data are combined from three experiments (n = 3). Significant differences from wt controls are designated by *$p < 0.05$.

(D) Ear skin sections were stained for histologic analysis (top rows) or with anti-CD68 mAb (bottom row). All scale bars, 40 μm.

disease at a slower rate when fed a standard chow diet (Breslow, 1996). A time course that charted the effects of age and the Western diet revealed that *Apoe*$^{-/-}$ lymph nodes (LNs) systemically became hypertrophic with age. This increase in LN cellularity was accelerated by feeding with a Western diet, such that LN hypertrophy was evident by 16 weeks of age in *Apoe*$^{-/-}$ mice fed a Western diet but was not evident until 34 weeks of age in chow-fed *Apoe*$^{-/-}$ animals (Figure 1A).

Loss of Skin DC Homeostasis Precedes the Onset of LN Hypertrophy

Systemic effects, such as skin inflammation, have been described in atherosclerotic mice (Feingold et al., 1995; van Ree et al., 1995). Considering the observed LN hypertrophy and the known skin inflammation, we focused on the possibility that skin DC were affected. *Apoe*$^{-/-}$ mice that were 6 weeks of age and maintained on a chow diet showed a uniform network of MHC II^{+} DCs in the epidermis at similar density as observed in wt mice (Figures 1B and 1C, top). However, at this relatively early age, the total number of Langerin^{+} epidermal DCs (Langerhans cells, LCs) in skin draining LNs was increased in *Apoe*$^{-/-}$ mice at 6 weeks of age, suggesting that LCs may be emigrating to LNs at a greater rate in *Apoe*$^{-/-}$ mice than in wt mice at this age (Figure 1C, bottom). Consistent with this possibility, there were 50% fewer LCs per mm^2 in *Apoe*$^{-/-}$ mice fed either a chow or a Western diet by 16 weeks, when the disease is well underway (Breslow, 1996) (Figures 1B and 1C, top). This loss reached a plateau such that later times examined were similar to 16 weeks. The ears of 34-week-old *Apoe*$^{-/-}$ mice fed a Western diet were too irritated and damaged to perform analysis. At and after 16 weeks of age, the number of LCs in the LN was decreased compared to wt mice (Figure 1C, bottom). Furthermore, by 16 weeks, independent of diet type, DCs that remained in the epidermis appeared activated compared to LCs from wt epidermis. Deconvolution imaging indicated that they expressed MHC II on the surface instead of in an intracellular perinuclear compartment, as usually seen in vivo (color panels, Figure 1B).

The age-dependent reduction in epidermal DCs in atherosclerotic mice suggests that developmental seeding of the epidermis with DCs was normal; that between 6 and 16 weeks of age, and therefore prior to LN hypertrophy, events in the skin caused some LCs to leave the epidermis and accumulate in LNs; and that the turnover of LCs was insufficient to meet demand for replacement.

Alterations in the Dermis of *Apoe*$^{-/-}$ Mice

We also observed a generalized increase in baseline ear thickness in *Apoe*$^{-/-}$ mice compared with wt counterparts. Histopathological analysis of ear sections from *Apoe*$^{-/-}$ mice and matched controls revealed no differences compared to wt at 6 weeks of age (Figure 1D). With time, *Apoe*$^{-/-}$ skin was affected by hyperkeratosis, spongiosis, and dermal accumulation of lymphohistiocytic cells (Figure 1D) consistent with a previous study (van Ree et al., 1995). These cells colocalized with scattered CD4^{+} cells and a few cells bearing LC markers like langerin (not shown). There were also notably increased numbers of CD68^{+} cells (Figure 1D) that would identify monocytes, macrophages, and some stages of DC maturation.

Skin DC Migration in *Apoe*$^{-/-}$ Mice Is Impaired by 16 Weeks of Age

Signs of activated LCs, dermal infiltration, and hypertrophic skin-draining LNs are consistent with the notion of immune activation in atherosclerosis. We hypothesized that the inflammatory environment in atherosclerotic mice activated skin DCs and promoted their mobilization to LNs, which in turn might facilitate subsequent LN hypertrophy. We thus studied DC migration by using a model based on the topical application of FITC in a contact-sensitizing solution that results in the appearance of FITC^{+} skin-derived DCs in the draining LNs. Compared to wt mice, 16 week-old *Apoe*$^{-/-}$ mice showed a significant decrease in the accumulation of FITC^{+} DCs in LNs independent of diet type (Figures 2A–2C). Wt mice fed a Western diet showed no differences in DC migration relative to chow-fed counterparts (data not shown).

These results were expressed as the percentage of FITC^{+} DCs in the LNs (Figure 2B) or as the number of FITC^{+} DCs in the LNs (Figure 2C). Both methods of calculation revealed that DC migration was inhibited in *Apoe*$^{-/-}$ mice fed a chow diet or a Western diet compared to wt mice. Because wt DCs migrate in greater numbers to larger LNs and indeed migrate into LNs in proportion to LN size (Supplemental Figure S1 available online at http://www.immunity.com/cgi/content/full/21/4/561/DC1/), normal DC migration is best appreciated as the percentage of FITC^{+} DCs. Thus, in many of the remaining experiments DC migration was expressed as the percentage of FITC^{+} DCs to eliminate independent variance due to differences in LN size/cellularity.

Examination of the epidermis from 16- and 34-week-old *Apoe*$^{-/-}$ mice fed a chow or a Western diet revealed a decreased percentage of LCs that migrated from the epidermis after FITC sensitization compared to an average loss of 35%–40% (150–200 cells/mm^2) in wt controls (Figure 2D). The possibility that the loss of DCs from the epidermis and even the failure of DCs to migrate to the LNs when probed at 16 or 34 weeks of age was related to the baseline reduction in epidermal DC density is unlikely because the migration of DCs after FITC application is not affected in other strains of mice, such as CD40L transgenic mice (Mehling et al., 2001) or op/op mice (Randolph et al., 1998a), which show a substantially reduced density of epidermal DCs (Witmer-Pack et al., 1993). Furthermore, as shown below, DC migration can be fully restored under conditions when DC density in the epidermis changes only minimally.

Inhibition of DC migration in atherosclerotic mice was also not explained by decreased expression of CCR7. Indeed, CCR7 mRNA was induced after FITC painting in wt mice at 6 and 16 weeks of age, and similar levels of CCR7 were detected in the epidermis of *Apoe*$^{-/-}$ mice when the mice developed disease (at 16 weeks of age) (Figure 2E). CCR7 expression was not altered (induced) in the steady-state epidermis of *Apoe*$^{-/-}$ mice, even when signs of inflammation and DC activation were present.

Finally, we confirmed that the decreased number of

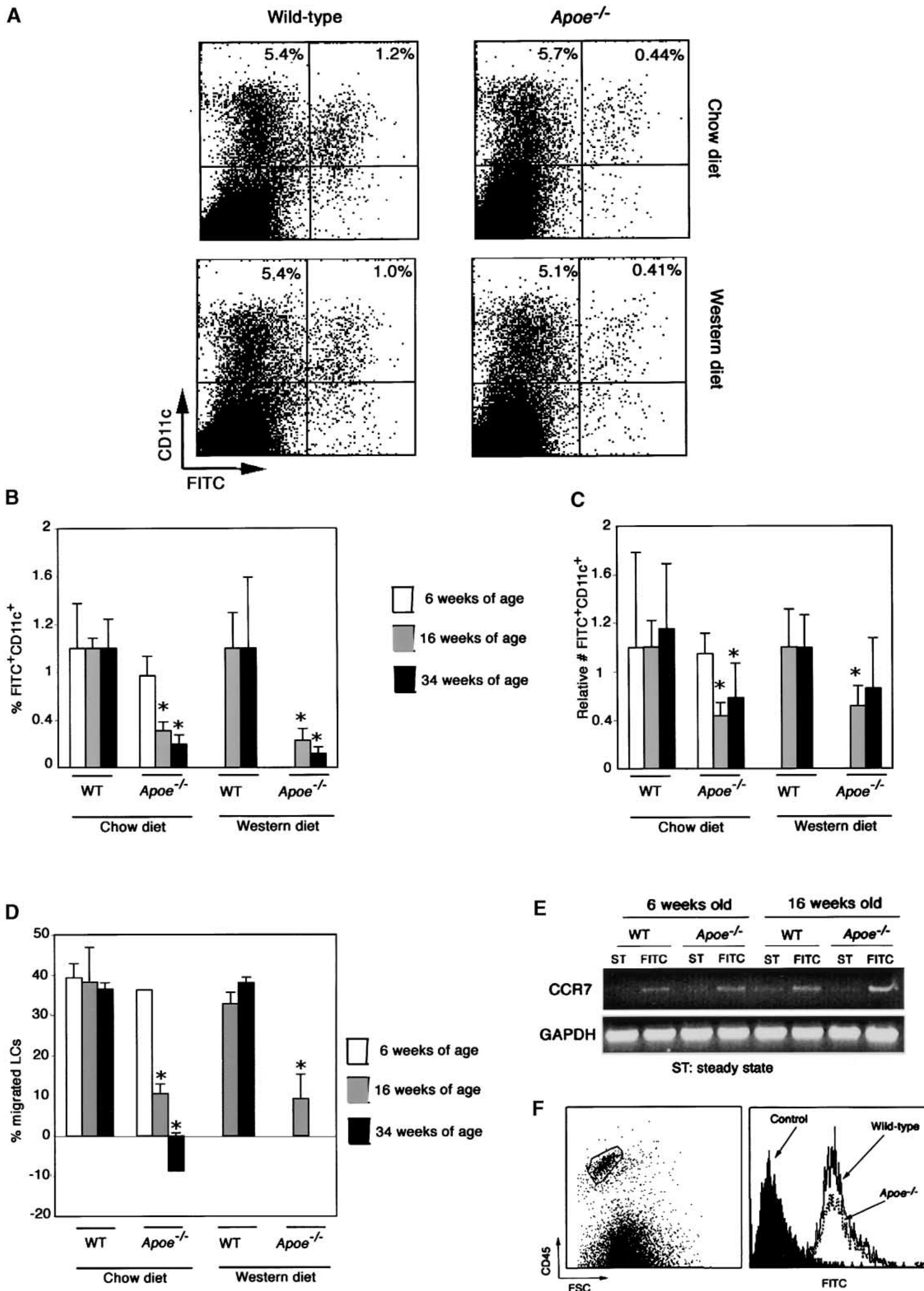

Figure 2. Analysis of DC Migration to Draining LNs in *Apoe*$^{-/-}$ Mice

(A) Wt and *Apoe*$^{-/-}$mice received epicutaneous FITC, and the accumulation of FITC^{+} cells (x axis) in the LNs was assessed. DCs were identified by using PE-conjugated anti-CD11c mAb (y axis).

(B) Percentage of FITC^{+}CD11c^{+} DCs in LNs from wt and *Apoe*$^{-/-}$ mice was determined (means of four experiments).

(C) To combine values from four independent experiments, the relative number of FITC^{+}CD11c^{+} DCs per LN for each data point in each experiment was calculated.

(D) Epidermal sheets from wt and *Apoe*$^{-/-}$ mice fed a chow or a Western diet were stained with anti-IA^{b} mAb after one ear was painted with FITC. Percentage of migrated LCs was calculated by comparing densities between painted and unpainted ears. Data are from four experiments.

(E) CCR7 mRNA expression in emigrated LCs from wt and *Apoe*$^{-/-}$ epidermis was assessed in the steady state and 18 hr after FITC painting.

(F) Epidermal suspension were prepared 18 hr after FITC application and stained with CD45. Gated CD45^{+} cells were analyzed for FITC content. Significant differences from wt controls are designated by *$p < 0.05$.

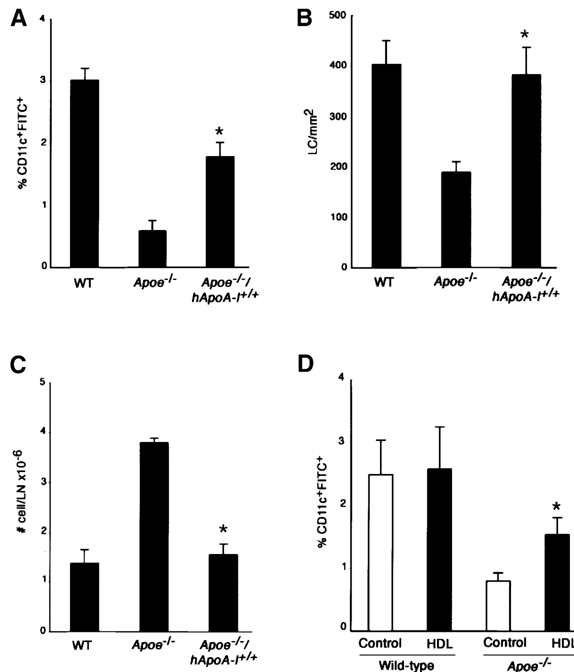

Figure 3. Effect of Elevating HDL on DC Migration in $Apoe^{-/-}$ Mice

(A) The accumulation of $FITC^{+}$ DCs in LNs after FITC painting, (B) the baseline LC density, and (C) LN cellularity were evaluated in wt, $Apoe^{-/-}$, and $Apoe^{-/-}/hApoA\text{-}I^{+/+}$ mice fed a Western diet for 10 weeks.

(D) Wt and $Apoe^{-/-}$ mice fed a Western diet for 10 weeks received i.v. 500 μg of human albumin (control) or HDL isolated from normal plasma (HDL) for 7 days before FITC application. One typical experiment is shown for each part of the figure. Each experiment was repeated three times with similar results. Significant differences from untreated $Apoe^{-/-}$ controls are shown; *$p < 0.001$.

$FITC^{+}$ DCs in LN from $Apoe^{-/-}$ mice did not result from impaired FITC uptake by skin DCs (Figure 2F). Indeed, the intensity of FITC expression on gated $CD45^{+}$ epidermal cells was not different between wt and $Apoe^{-/-}$ mice. Altogether, these data illustrate that DC migration to LNs is impaired in $Apoe^{-/-}$ mice by 16 weeks of age, a time when progression of atherosclerosis is well underway in both chow and Western diet-fed animals (Breslow, 1996), but not in younger 6-week-old mice that have minimal manifestations of disease. This inhibitory effect of DC migration was associated with atherosclerotic disease in other murine models of atherosclerosis, since we observed similar results in $Ldlr^{-/-}$ mice (Supplemental Figure S2).

HDL Prevents Alterations in DC

Elevating HDL-cholesterol levels can reverse progression of atherosclerotic disease (Rong et al., 2001). We wondered if raising HDL might reverse changes observed for skin DCs. Therefore, we evaluated DC migration in $Apoe^{-/-}$ mice that transgenically express human ApoAI ($Apoe^{-/-}/hApoA\text{-}I^{+/+}$), the major apoprotein of HDL. Expression of this transgene leads to elevated HDL levels (Plump et al., 1994; Schultz et al., 1993). In $Apoe^{-/-}/hApoA\text{-}I^{+/+}$ mice, DC migration was not equivalent to wt mice but was significantly improved over $Apoe^{-/-}$ mice lacking this transgene (Figure 3A). Furthermore, shifts in DC density in the epidermis (Figure 3B) and LN cellularity (Figure 3C) were not observed in $Apoe^{-/-}/hApoA\text{-}I^{+/+}$ mice, in contrast to $Apoe^{-/-}$ mice.

These data suggest that elevating HDL from birth quells the onset of alterations in skin DCs and LN hypertrophy. However, studies in these transgenic mice are inherently unable to delineate whether HDL could reverse the observed alterations in DC function and LN hypertrophy once established. To begin to address this question, wt and $Apoe^{-/-}$ mice were treated intravenously (i.v.) with 500 μg HDL isolated from normal human plasma every day for 7 days. On the last day of treatment, the skin of these mice was painted with FITC, and the extent to which $FITC^{+}CD11c^{+}$ DCs accumulated in the LNs was determined. In wt mice, treatment with HDL had no effect on the accumulation of $FITC^{+}$ DCs in the LNs compared to mice receiving only PBS (Figure 3D). In contrast, HDL injection in $Apoe^{-/-}$ mice partially restored migration of $FITC^{+}$ DCs to LNs, increasing the fraction of $FITC^{+}CD11c^{+}$ DCs in draining LNs compared to nontreated $Apoe^{-/-}$ mice by 50%. This correction by HDL was related to a slight decrease in total cholesterol and increase in HDL-cholesterol in plasma from $Apoe^{-/-}$ mice compared to untreated $Apoe^{-/-}$ mice (Table 1). The transfer of HDL to wt mice did not affect their plasma lipid profiles (Table 1). Thus, short-term treatment with HDL partially reverses the impaired DC mobilization to LNs that is blocked in $Apoe^{-/-}$ mice.

PAFAH Is a Component of HDL Required to Maintain Normal DC Migration

HDL is enriched in proteins that scavenge oxidized molecules, including in particular PAFAH (Marathe et al., 2003). Plasma PAFAH activity is critical for the inactivation of PAF and PAF-like lipids associated with oxidized LDL (Forte et al., 2002), and gene therapy approaches that raise the level of PAFAH decrease the progression of atherosclerosis (Quarck et al., 2001). Since we have noticed a migration inhibitory effect on DCs by PAF signals in other models (Llodra et al., 2004), we wondered whether the PAFAH endogenously associated with HDL accounted for the migration restorative effect of HDL. First, wt and $Apoe^{-/-}$ mice maintained on a Western diet for 12 weeks received i.v. for 7 consecutive days 500 μg HDL isolated from plasma from a normal donor or from individuals bearing an inactivating mutation in the PAFAH gene (Stafforini et al., 1996). An analysis of PAFAH activity confirmed that this HDL was deficient in PAFAH activity (Figure 4A). In wt mice, treatment with HDL containing active or mutated PAFAH had no effect on $FITC^{+}$ DC accumulation in the draining LNs (data not shown). In contrast, in $Apoe^{-/-}$ mice, HDL containing active PAFAH partially restored DC migration and did so much more effectively than HDL lacking functional PAFAH (Figure 4B).

In further experiments, HDL isolated from normal human plasma was treated with an irreversible serine protease inhibitor, Pefabloc (Dentan et al., 1996), which reduced PAFAH activity associated with HDL by 85% (Figure 4A). Then, wt and $Apoe^{-/-}$ mice fed a Western diet were treated i.v. with 500 μg HDL containing active or biochemically inactivated PAFAH for 7 consecutive days. Again, the modulation of PAFAH activity in this

Table 1. Effect of HDL Treatment on Blood Lipid Profiles

	Treatment	Total Cholesterol (mg/dl)	HDL Cholesterol (mg/dl)
Wild-type	None	116.5 ± 31.8	54 ± 4.24
	HDL	94 ± 4.2	43.5 ± 10.6
Apoe$^{-/-}$	None	1896 ± 46.66*	29.5 ± 2.12
	HDL	1528 ± 210.3*	63.3 ± 18

Values are mean ± SD. *p ≤ 0.1. All mice were fed a Western diet for 12 weeks.

manner had no effect on DC migration in wt mice (data not shown). Treatment with HDL containing active PAFAH reversed the inhibitory effect on DC migration in *Apoe*$^{-/-}$ mice (Figure 4C). In contrast, accumulation of FITC^{+} DCs in LNs was only modestly increased over untreated *Apoe*$^{-/-}$ mice when *Apoe*$^{-/-}$ mice received

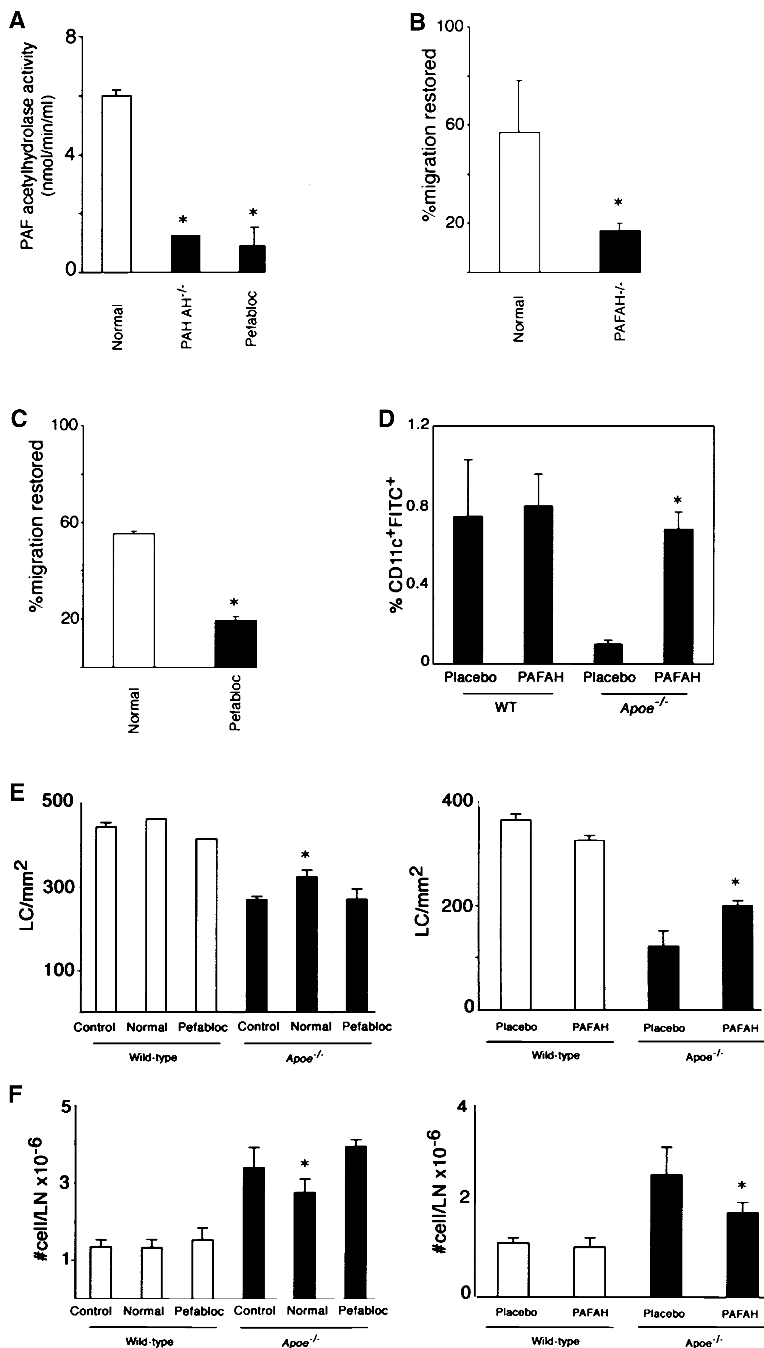

Figure 4. Role of HDL-Associated PAFAH in DC Migration

(A) PAFAH activity was measured in HDL isolated from normal plasma (normal), in HDL derived from individuals who are homozygous deficient for PAFAH (PAFAH$^{-/-}$), or in HDL from normal plasma treated with the Pefabloc (Pefabloc).

(B) The effect of normal HDL (Normal), PAFAH-deficient HDL (PAFAH$^{-/-}$), or (C) Pefabloc-inactivated PAFAH HDL (Pefabloc) treatment on DC migration was analyzed in *Apoe*$^{-/-}$ mice fed a Western diet after FITC painting. The results are expressed as the percentage of migration restored, where 100% reversal is defined as the difference between the percentage of FITC^{+} DC in untreated wt and *Apoe*$^{-/-}$ mice.

(D) Wt or *Apoe*$^{-/-}$ mice kept on the Western diet received 0.1 mg/kg i.v. of placebo (Placebo) or recombinant PAFAH (PAFAH) for 7 consecutive days before FITC painting.

(E) Wt and *Apoe*$^{-/-}$ mice kept on the Western diet for 10 weeks were treated with normal HDL (Normal), Pefabloc-inactivated PAFAH HDL (Pefabloc), or recombinant PAFAH (PAFAH). Baseline LC density was determined by immunostaining with anti-IA^{b} mAb.

(F) Total cells numbers in skin draining LNs were evaluated. Data are combined from three experiments. Significant differences are designated by *p < 0.05.

HDL containing inactivated PAFAH (Figure 4C). These results indicate that the restoration of DC migration mediated by HDL in large part depends on its PAFAH activity.

We next investigated whether administration of recombinant PAFAH for 7 consecutive days would restore DC migration in *Apoe*$^{-/-}$ mice. Indeed, the fraction of migrating DCs in the draining LNs from *Apoe*$^{-/-}$ mice treated with recombinant PAFAH was almost totally restored to wt levels (Figure 4D).

We wondered whether this treatment might also have some impact on LC density that is altered in *Apoe*$^{-/-}$ mice (Figure 1). Compared to untreated *Apoe*$^{-/-}$ mice, the number of LC/mm^2 began to show increases toward wt density after both HDL and PAFAH treatments (Figure 4E). There were also slight reductions in the cellularity of the LNs (Figure 4F). Since PAFAH treatment fully restored DC migration but only modestly affected epidermal DC density and LN cellularity during 7 days, the data indicate that correcting to normal the impaired DC migration is not dependent on full correction of the other alterations.

HDL-Associated PAFAH Maintains Normal Immune Responses

The development of immune responses is severely compromised in *Apoe*$^{-/-}$ mice (de Bont et al., 1999; Laskowitz et al., 2000; Ludewig et al., 2001). Reversing the inhibitory effect on DC migration observed in *Apoe*$^{-/-}$ mice might have some direct consequences on the capacity of these mice to elicit immune responses since migration of DC from the site of antigen entry to the draining LN is required to induce immune responses like contact hypersensitivity (CHS) and delayed-type hypersensitivity (DTH) (Flores-Romo, 2001).

We first confirmed that CHS and DTH elicited with FITC and OVA, respectively, were depressed in *Apoe*$^{-/-}$ mice at 16 weeks of age (Western diet for 10 weeks). *Apoe*$^{-/-}$ mice mounted greatly reduced CHS and DTH responses (70% and 50% inhibition, respectively) compared with sensitized wt mice (Figures 5A and 5B). *Apoe*$^{-/-}$ mice treated with either HDL from normal human serum or recombinant PAFAH mounted a stronger CHS response compared with untreated *Apoe*$^{-/-}$ mice that was near to wt levels (Figure 5A), but administration of PAFAH-inactivated HDL in *Apoe*$^{-/-}$ mice had no beneficial effect on the CHS response. Similarly, restoration of DC migration by recombinant PAFAH in *Apoe*$^{-/-}$ mice improved the DTH responses induced by OVA in these mice (Figure 5B). The expression of costimulatory molecules on LN DCs from *Apoe*$^{-/-}$ mice was similar to wt DCs (Figure 5C). DCs were not fully mature in the absence of FITC painting. After FITC painting, the fewer number of FITC$^+$ DCs in *Apoe*$^{-/-}$ LNs had matured like their more numerous wt FITC$^+$ counterparts. These data indicate that impaired DC migration rather than alterations in DC maturation largely account for the altered immune responses in *Apoe*$^{-/-}$ mice.

PAF-Derived Signals Negatively Regulate DC Migration

The role of PAFAH in restoring DC migration in *Apoe*$^{-/-}$ mice suggests that PAF or PAF-like lipids arising in atherosclerotic disease by oxidation of LDL or generated in the course of inflammation in skin may negatively regulate skin DC migration through PAF receptor (PAFR). This receptor is expressed by human DCs (Dichmann et al., 2000; Sozzani et al., 1997). We detected PAFR mRNA in mouse LCs that emigrated from cultured skin explants and in bone marrow-derived DCs (BMDCs) from wt mice (Figure 6A). Thus, we investigated DC migration in *Pafr*$^{-/-}$ mice (Ishii et al., 1998; Ishii and Shimizu, 2000). After FITC application, the fraction and the total number of FITC$^+$CD11c$^+$ DCs in *Pafr*$^{-/-}$ mice LNs were essentially doubled compared with wt (Figure 6B). This enhanced migration was associated with a loss of skin DCs, but the baseline density of LCs in *Pafr*$^{-/-}$ mice was similar to wt mice (data not shown). Interfering in vivo with PAFR by using the specific antagonist CV3988 also increased DC migration in wt mice, but less substantially than the increases observed in PAFR-deficient mice (Figure 6C). These data support the idea that PAF signals normally negatively regulate DC migration in vivo, even curtailing migration in *Apoe*$^{+/+}$ mice subjected to an activation stimulus.

To test whether PAF signals act directly on DCs to modulate their migration, we adoptively transfered wt or *Pafr*$^{-/-}$ CD45.2 BMDCs to wt congenic CD45.1 recipients, or conversely, BMDCs from wt congenic CD45.1 mice were transferred to wt or *Pafr*$^{-/-}$ recipients. Migration of DCs to skin draining LNs was analyzed two days later. DC migration to recipient LNs was twice greater for *Pafr*$^{-/-}$ BMDCs compared with wt BMDCs (Figure 6D). In contrast, the migration of wt BMDCs was not different between wt and *Pafr*$^{-/-}$ recipients (Figure 6D). Thus, signals through PAFR expressed by DCs themselves can serve to negatively regulate mobilization from skin to LNs.

These observations in mice appear to be relevant to human skin DCs. First, human LCs that emigrated from skin explants also expressed PAFR mRNA and fluxed calcium in response to cPAF (Figure 6E), a specific stable agonist of the PAFR (O'Flaherty et al., 1987). Furthermore, the addition of the PAFR antagonist CV3988 enhanced LC emigration from skin explants, as much as IL-1β (Figure 6E). Treatment with CV3988 affected neither CCR7 nor costimulatory molecule expression on LCs (data not shown).

Discussion

Here, we show that the dyslipidemia associated with atherosclerosis markedly modifies DC functions in skin. The presence and migration of DCs in skin are normal up through 6 weeks of age. Therefore, the absence of *Apoe* per se does not noticeably modify DC seeding of the epidermis, LN development, or DC migration. However, by 16 weeks of age, when hypercholesterolemia is marked, there is an evident loss of LCs, and those that remain in the epidermis appear activated, expressing MHC II at the plasma membrane instead of retaining it in a perinuclear deposition that characterizes immature DCs. Considering the increased number of LCs in the draining LN of *Apoe*$^{-/-}$ mice at 6 weeks of age, the data suggest that migration of DCs out of the epidermis is stimulated early in the disease before 16 weeks.

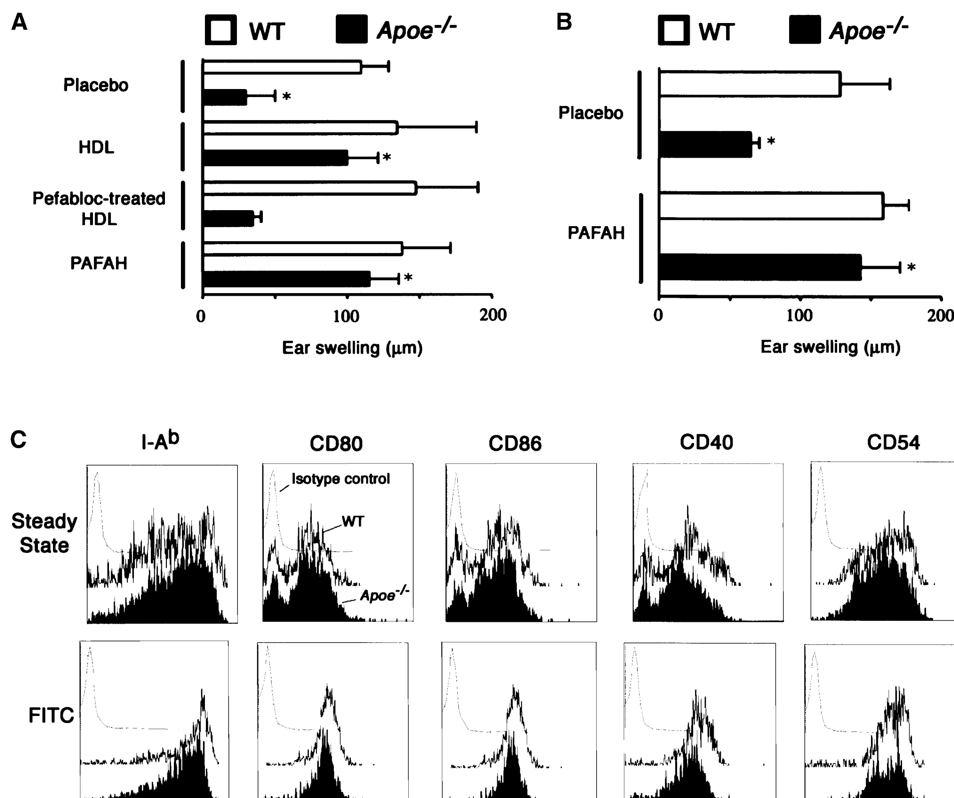

Figure 5. Effect of PAFAH-Associated HDL on Immunologic Parameters in $Apoe^{-/-}$ Mice

Wt and $Apoe^{-/-}$ mice kept on the Western diet for 10 weeks were treated with HDL, Pefabloc-inactivated HDL, or recombinant PAFAH for 7 consecutive days before sensitization and one day after sensitization. (A) CHS and (B) DTH responses were assessed and expressed as ear swelling. Baseline unchallenged ear thickness was 40 $\pm$ 2 μm in wt mice and 50 $\pm$ 5 μm in $Apoe^{-/-}$ mice. (C) Expression of costimulatory molecules on CD11c^{+} DCs (steady state) or on CD11c^{+}FITC^{+} DCs (18h FITC painting) was assessed by flow cytometry in LNs from wt (unfilled histograms) and $Apoe^{-/-}$ mice (filled histograms) at 16 weeks of age and fed a Western diet. Results shown are from one experiment typical of three conducted. Significant differences from wt controls are designated by *$p < 0.01$.

By 16 weeks, in contrast, migration of DCs to the LN was impaired in $Apoe^{-/-}$ and in $Ldlr^{-/-}$ mice. This defect was associated with poor priming of CHS and DTH responses, consistent with impaired immunity in atherosclerotic mice previously noted by others in a variety of challenges (de Bont et al., 1999; Ludewig et al., 2001; Netea et al., 1997; Roselaar and Daugherty, 1998; Van Lenten et al., 2002). Poor contact sensitization was not due to reduced numbers of epidermal DCs, because treatment with PAFAH nearly fully restored migration, but increased DC density in the epidermis more slowly. Moreover, other studies in which LCs are activated by expression of CD40L in the skin show that a partial loss in LCs does not result in apparent inhibition of migration after FITC application (Mehling et al., 2001). Despite poor migration and consequently poor priming from the periphery, $Apoe^{-/-}$ and $Ldlr^{-/-}$ LNs nonetheless become markedly enlarged, a sign that is often considered a hallmark of autoimmunity in mice.

Thus, DC migration and immune priming are impaired even as systemic activation of LNs and skin DCs are apparent. In vivo it is unusual to observe epidermal DC activation even after sensitization. Skin-localized, activated DCs might participate in the production of cytokines like IL-1 and TNFα (McLachlan et al., 2003) and chemokines (Palframan et al., 2001) that drain to the LN and, in “remote control” fashion, promote influx of cells through high endothelial venules. These mediators produced by local DCs could also directly attract additional cells to the skin. Therefore, our data are consistent with the possibility that at earlier points in the disease, DCs may migrate in response to spontaneous activation and could prime responses to antigens such that later, when further capacity for priming is impaired, memory responses may persist unabated, as memory T cells would likely traffic to the periphery where DCs are found. Indeed, impaired migration of DCs from the periphery may even aid in further localizing and exacerbating memory responses to the periphery, enhancing local tissue reactions.

When $Apoe^{-/-}$ and $Ldlr^{-/-}$ mice are immunologically challenged, they show impaired priming and reduced capacity for clearance of bacteria (de Bont et al., 1999; Roselaar and Daugherty, 1998), fungi (Netea et al., 1997), and virus (Ludewig et al., 2001). Where time courses have been conducted, susceptibility to infection does not occur in younger mice but increases with age and diet (Ludewig et al., 2001; Moazed et al., 1997), consis-

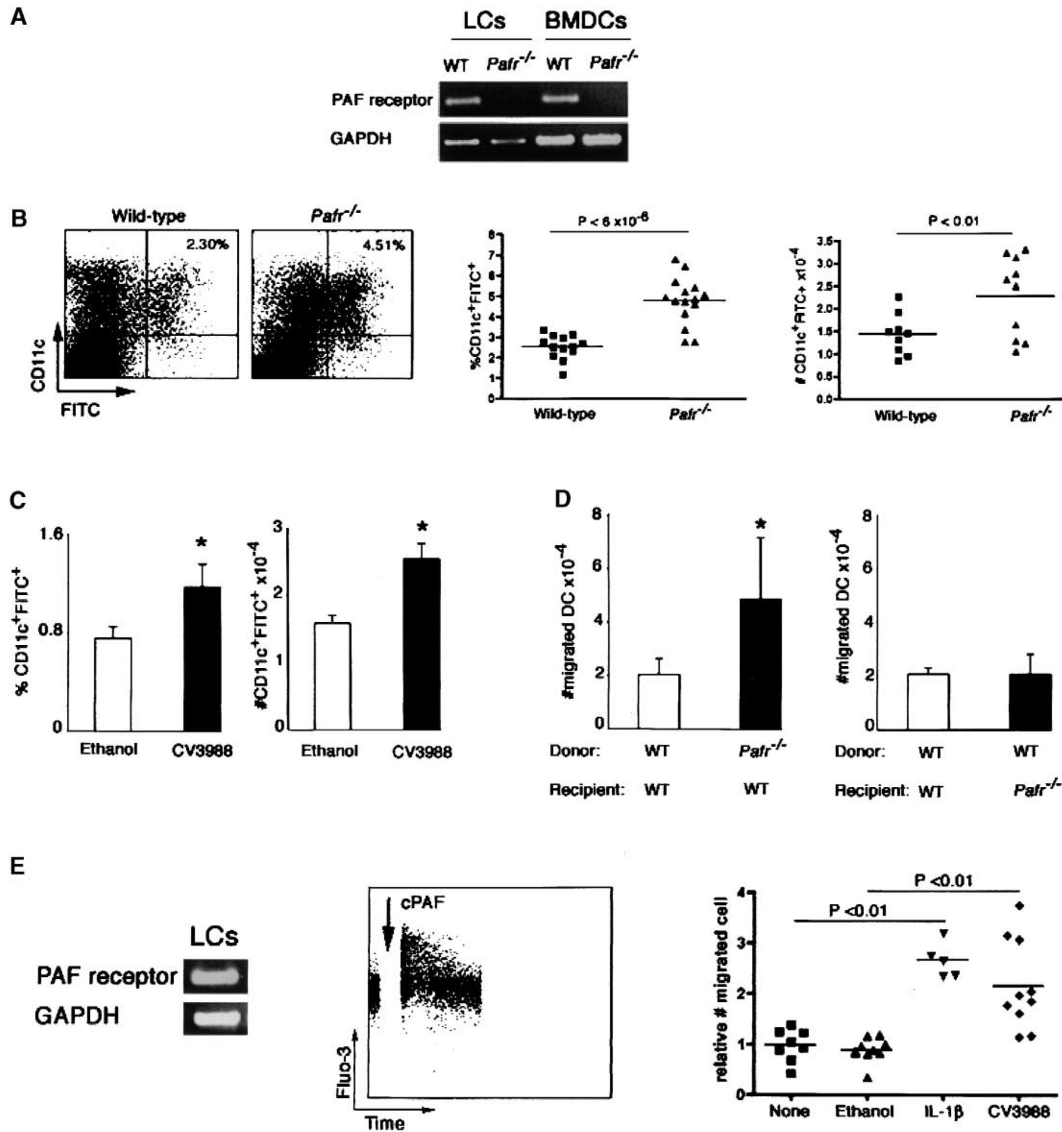

Figure 6. PAFR Expression and Function during DC Migration

(A) Expression of mRNA for PAFR by wt and $Pafr^{-/-}$ LCs emigrated from skin explants and by wt and $Pafr^{-/-}$ BMDCs was assessed.

(B) After FITC application on skin of wt and $Pafr^{-/-}$ mice, $FITC^{+}$ $CD11c^{+}$ cells in LNs were analyzed. Percent and total number of $FITC^{+}CD11c^{+}$ DCs in LNs from wt and $Pafr^{-/-}$ mice were determined. Data points are pooled from two experiments.

(C) Migration of DCs after FITC painting was assessed in wt mice treated with the PAFR antagonist CV3988 or ethanol (control solvent) 1 day before and the day of FITC painting.

(D) Adoptive transfer of BMDCs from WT or $Pafr^{-/-}$ CD45.2 mice (donor) was performed in the back skin of wt CD45.1 recipients, or conversely, BMDCs from wt CD45.1 mice (donor) were transferred to wt and $Pafr^{-/-}$ CD45.2 recipients. 2 days after cell transfer, the number of DC that migrated to brachial LNs was determined. All results are representative of at least two experiments ($n \geq 4$). Significant differences are designated by $*p < 0.05$.

(E) Expression of mRNA for PAFR in human LCs was analyzed (left). Calcium flux in human LCs was measured in response to cPAF. Arrow indicates point of cPAF addition (middle). Culture medium of human skin explants was supplemented with IL-1β, CV3988, its control solvent (ethanol), or with no additives. Emigration was quantified after 24 hr (right). Data points represent normalized emigration from individual 4 cm^2 explants.

tent with the later onset of impaired DC migration. It has been suggested that association of human atherosclerosis with *Chlamydia pneumoniae* and cytomegalovirus infection may be related to ill management of these pathogens in the disease (Ludewig et al., 2001) in addition to the often discussed possibility of a causative role of the pathogens in promoting atherosclerosis (Zebrack and Anderson, 2003; Ludewig et al., 2004) and other autoimmune disorders (Sekigawa et al., 2002). By illustrating that DCs poorly prime because they migrate inefficiently to LNs but remain activated in the periphery, our data can reconcile the current paradox regarding

how mediators of innate immunity and signals from pathogens (Bjorkbacka et al., 2004) or apoptotic debris (Aprahamian et al., 2004) might lead to exacerbation of local inflammation, autoimmunity, and atherosclerosis that is coexistent with suppressed immune priming.

Mechanisms of Impaired Migration by PAFAH Substrates: Mediation through PAFR and Other Possible Pathways

We show that HDL, and particularly HDL containing active PAFAH, or recombinant PAFAH can reverse impaired *Apoe*$^{-/-}$ DC migration, and restore immunologic priming. These agents have long been known for their anti-inflammatory properties (Rong and Fisher, 2000; Tjoelker and Stafforini, 2000). The protective effect of HDL results in part from its association with PAFAH. Individuals that bear an inactivating mutation in the PAFAH gene manifest increased incidence of coronary heart disease (Yamada et al., 1998). A recent study revealed that an HDL mimetic could reverse the susceptibility of *Ldlr*$^{-/-}$ mice to influenza infection (Van Lenten et al., 2002). Our studies agree with the idea that HDL supports a healthy, protective immune response, and suggest that one mechanism by which it does so is through PAFAH activity that maintains normal DC migration.

It is not yet clear whether the key target of PAFAH in these studies is oxidized LDL that can act as a PAF mimetic or PAF itself that would be produced during skin inflammation. That epidermal DCs in *Apoe*$^{-/-}$ mice exhibited a more-activated phenotype is consistent with a role for oxidized LDL in inducing DCs maturation (Alderman et al., 2002). Since both PAF-like oxidized LDL and PAF bind to PAFR expressed on skin DCs, they may each exhibit similar capacity to impair DC migration. Elimination of PAF signaling in *Pafr*$^{-/-}$ mice led to significantly increased DC migration even in *Apoe*$^{+/+}$ mice, and these effects were mediated directly through the activation of PAFR on DCs. This finding implies that PAF production at inflammatory sites serves as a means to normally curtail DC migration.

Thus, our data are consistent with a model in which PAF-like lipids, which build-up systemically in atherosclerotic mice, impair DC migration by signaling through PAFR. However, other mechanisms may also apply. A broad spectrum of chemokines, including the CCR7 ligands CCL19 and CCL21, can act as soluble scavenger receptors in vitro (Shimaoka et al., 2004). Binding of these chemokines to scavenger receptor ligands, such as oxidized LDL, reduce their chemotactic activity by interfering with chemokine-chemokine receptor binding. Interestingly, the inflammatory chemokines CXCL8, CCL2, and CX_3CL1 are not recognized by oxidized LDL. Thus, the authors suggest, "The lack of OxLDL binding activity in CX_3CL1 and CCL2 may allow these chemokines to exhibit chemotactic activity toward targeted leukocytes in atherosclerotic lesions even in the presence of high local concentrations of OxLDL. Conversely, OxLDL may suppress various immune reactions by binding to various chemokines." This prediction fits nicely with our in vivo findings. This model, in which impaired DC migration might result from scavenging of chemokine activity, is inherently independent of PAFR biology. Future studies are needed to determine whether PAFAH might abrogate the scavenger receptor-like recognition between oxidized LDL and chemokines like CCR7 ligands and whether this mechanism plays a complementary role with negative regulatory signals through PAFR itself in affecting DC migration in dyslipidemic mice.

Relevance to the Advance of Atherosclerotic Plaques

Impaired DC emigration from skin parallels impeded migratory clearance of monocyte-derived DC-like cells from atherosclerotic plaques (Llodra et al., 2004). Thus, in analogy to observations in skin, maintaining the ability of DCs, which are abundant in lesions (Bobryshev et al., 2001), to undergo migratory clearance from lesions may diminish plaque size through the clearance of cell mass and from the removal of potentially activated, cytokine-producing cells that may promote further recruitment and retention of other cell types. Overexpression of human *ApoA-I* (Rong et al., 2001) or gene therapy approaches to promote overexpression of PAFAH (Quarck et al., 2001) lead to regression/stabilization of atherosclerotic lesions in mice. These are the same conditions that reverse impaired DC migration from the skin. Interestingly, in *Apoe*$^{-/-}$/*hApoA-I*$^{+/+}$ mice, monocyte recruitment to the lesion is not clearly diminished in these mice (Dansky et al., 1999), despite that the fact that overall lesion size remains lower than in controls. A possible explanation is that clearance of monocyte-derived DC-like cells out of the lesion (Llodra et al., 2004) may be promoted by HDL. Thus, the actions of HDL in promoting DC migration may diminish the advance of atherosclerotic lesions while also generally maintaining homeostasis and normal responsiveness in the DC compartment systemically.

Experimental Procedures

Mice

Female and male wt mice (CD45.2 and CD45.1) C57BL/6, C57BL/6 deficient for apolipoprotein E (*Apoe*$^{-/-}$), and LDL receptor (*Ldlr*$^{-/-}$) mice were obtained from Jackson Laboratory. Mice deficient for PAF receptor (*Pafr*$^{-/-}$) and *Apoe*$^{-/-}$ transgenic for human ApoA-I (Apoe$^{-/-}$/*hApoA-I*$^{+/+}$) fully backcrossed on C57BL/6 background have been previously described (Ishii et al., 1998; Ishii and Shimizu, 2000; Plump et al., 1994). Animals were maintained on a chow diet or switched at 6 weeks of age to a high-fat Western diet (21% milk fat and 0.15% cholesterol; Harlan-Teklad laboratory) for 10 or 28 additional weeks corresponding to 16 and 34 weeks of age, respectively. All studies were approved by the Institutional Animal Care and Use Committee at Mount Sinai School of Medicine.

DC Migration Assay

Epicutaneous application of FITC to study DC migration was performed on the ears and/or on three areas of each side of the mice that drain to axillary, brachial, and inguinal LNs as described (Robbiani et al., 2000). These LNs were recovered 18 hr later, digested in collagenase D, and pressed through a 70 μm cell strainer. The total cell number was evaluated for each sample by using a hemacytometer, and samples were analyzed by flow cytometric analysis by staining with PE-conjugated anti-CD11c mAb (Becton Dickinson Biosciences) and with biotinylated anti-I-A^b, CD80, CD86, CD54, or CD40 mAbs (Becton Dickinson) detected by allophycocyanin-conjugated streptavidin.

Quantification of Migration

To quantify the number of LCs in the steady state LN, permeabilized LN suspensions were stained with langerin mAb (provided by Dr S. Saeland, Schering Plough) and PE-conjugated anti-rat mAb (Jack-

son Immunoresearch). To quantify migration of DCs induced by FITC application, the percentage of FITC$^+$CD11c$^+$ DCs in the total LN population was assessed by flow cytometry. Expression of data as the percentage of FITC$^+$ DCs eliminates unrelated variance due to differences in LN size/cellularity (Supplemental Figure S1). Alternatively, the total number of FITC$^+$CD11c$^+$ DCs per LN was calculated by multiplying the percentage of FITC$^+$CD11c$^+$ cells by the number of total LN cells. To compare results from different experiments, relative values for individual data points were in some cases generated by dividing the value of a data point by the mean of the wt control from the same experiment.

Preparation of Epidermal Sheets and Suspensions

Epidermal sheets prepared as described (Angeli et al., 2001) were stained with anti-I-A^b mAb (BD Biosciences), followed by Cy3-conjugated anti-mouse mAb (Jackson Immunoresearch). Deconvolved images showing localization of MHC class II on LCs were acquired and analyzed by using Openlab and Volocity 2.0 software, respectively (Improvision, Inc.). The number of DCs that migrated out of the skin was enumerated by counting MHC class II-positive cells that remained in epidermis 18 hr after FITC application, compared with the baseline DC density obtained from epidermis to which no FITC was applied. Five random fields were quantified per sheet. To measure FITC uptake by epidermal cells, cell suspensions from wt and *Apoe*$^{-/-}$ mice were prepared as described (Randolph et al., 1998b) 18 hr after FITC application on the ears. Cells were stained with PE conjugated anti-CD45 mAb (BD Biosciences), and expression of FITC on gated CD45$^+$ cells was analyzed by flow cytometry.

Histology and Immunohistochemistry

Skin was snap-frozen in OCT compound and 8 μm sections were prepared and fixed in 100% acetone for 5 min. For immunohistochemistry, sections were blocked with Fc block (BD Biosciences) or 5% goat serum for 10 min. Primary antibodies used included anti-CD68 (Serotec) and biotinylated anti-CD4 (BD Biosciences). Cy3-conjugated streptavidin (Sigma) or Cy3-conjugated donkey anti-rat mAb (Jackson Immunoresearch) was used for detection.

Administration of Human HDL or Recombinant PAFAH

HDL (1.063–1.21g/ml) was isolated by ultracentrifugation (Havel et al., 1955) from normal plasma or from plasma derived from individuals who are homozygous deficient for PAFAH. After dialysis against PBS containing 2 mM EDTA, HDL preparations were sterilized through a 0.22 μm filter and stored under argon at 4°C. Protein content was determined (BCA kit, Pierce). Mice were treated with 500 μg of human albumin (control) or HDL by daily injection into the tail vein for 7 days. For inactivation of HDL-associated PAFAH, HDL (2.5 mg/ml) isolated from normal plasma was preincubated for 30 min at 37°C with 100 μM Pefabloc (Roche) and then immediately dialyzed in PBS-EDTA (Dentan et al., 1996). PAFAH activity was measured by using a kit from Cayman. In some experiments, mice were treated with 0.1 mg/kg of recombinant PAFAH (provided by ICOS Corporation) or placebo (its solvent control) by daily injection into the tail vein for 7 days.

Measurement of Plasma Lipids

HDL fractions were isolated from mouse plasma samples by density gradient ultracentrifugation. Total cholesterol and HDL-cholesterol were analyzed with commercial kits (Sigma).

Contact Hypersensitivity and Delayed-Type Hypersensitivity Responses

For contact hypersensitivity (CHS) response, mice were sensitized by painting 20 μl of a 0.5% solution of FITC prepared in acetone/dibutylphtalate on the total surface of the left ear. CHS was elicited 5 days after sensitization by painting dorsal and ventral surfaces of the right ear with 10 μl of 0.5% solution of FITC (Angeli et al., 2001). Ear thickness was measured by using a micrometer 24 hr after challenge. Results are expressed as ear swelling, which was calculated by subtracting the thickness of the ear before the challenge from its thickness after the challenge. For DTH, mice were sensitized by subcutaneous (s.c.) injection with 20 μg of OVA (Sigma) in the left ear. Delayed-type hypersensitivity (DTH) was elicited 10 days after sensitization by s.c. injection into the right ear with 30 μg of OVA (adapted from [Itano et al., 2003]). Results are expressed as ear swelling as described for CHS. In both CHS and DTH models, mice were treated with placebo, HDL, pefabloc-treated HDL, or recombinant PAFAH for 7 consecutive days before and one day after the sensitization (only during the day of DC migration).

RT-PCR

Total RNA was isolated from murine LCs that had emigrated from epidermal sheets of wt and *Pafr*$^{-/-}$ mice ears as described (Schuler and Steinman, 1985), from wt or *Pafr*$^{-/-}$ bone marrow-derived DCs, or from human LCs obtained as described below. cDNA was synthesized from 1 μg of total RNA with random hexamer primers and Superscript reverse transcriptase (Life Technologies). PCR amplifications were performed for 29 cycles with the primer pairs: GAPDH (453bp), 5′-ACCACAGTCCATGCCATCAC-3′ (forward) and 5′-TCCACCACCCTGTTGCTGTA-3′ (reverse); mouse PAFR (200 bp), 5′-TTGCCTGAGCCATCCTTATT-3′ (forward) and 5′-CCTCCCACTGTGGATTGTCT-3′ (reverse); human PAFR (300bp), 5′-ATGACTCCTCCCACATGGAC-3′ (forward) and 5′-GCAGGGTGATCAAGAAGAGC-3′ (reverse). Mouse and human CCR7 primers were from R&D Systems.

PAF Receptor Antagonist Administration

Wt mice were treated intraperitoneally (i.p.) with 20 mg/kg PAFR antagonist CV6988 (Biomol) (Montrucchio et al., 2000), or its solvent control (100% ethanol) one day before and the day of FITC application. Migration of DCs to the LNs was assayed 18 hr later as described above.

Bone Marrow-Derived DCs

BMDCs from wt congenic CD45.2$^+$, CD45.1$^+$, or *Pafr*$^{-/-}$ (CD45.2) mice were prepared as described (Robbiani et al., 2000) and used at day 8 of culture. DCs (0.8×10^6) from wt or *Pafr*$^{-/-}$ mice were injected in each side of the back skin of congenic CD45.1 recipients. Alternatively, DCs from congenic CD45.1 mice were injected into wt or *Pafr*$^{-/-}$ recipients. On the day of DC injection and one day after, recipient mice were painted with 50 μl of acetone: dibutylphtalate to mimic the usual FITC painting assay. 2 days later, migrated DCs in brachial LNs were analyzed with PE-conjugated anti-CD11c mAb and biotinylated anti-CD45.1 or CD45.2 mAb (Southern Biotech) and detected with allophycocyanin-conjugated streptavidin for analysis by flow cytometry.

Human Skin Explants and Calcium Flux

Human split-thickness skin explants obtained from organ donors within 34 hr of death (New York Firefighter's Skin Bank, Cornell University) were cultured in medium containing 10 μM CV3988, its solvent control (100% ethanol), 1 μg/ml of IL-1β (R&D Systems), or no additives and analyzed as described previously (Randolph et al., 1998b). Cells were quantified 1 day later.

For calcium flux, emigrated LCs were loaded with FLUO-3 (Molecular Probe, 5 μM) and resuspended to 0.5×10^6 cell/ml in PBS containing 0.03%BSA. After collecting events for several seconds to establish baseline, 100 nM of carbamyl PAF (Biomol) was added to the cells and fluorescence was monitored for 2 min by flow cytometry.

Statistics

Statistical comparisons were made by using the Student's two-tailed t test. Results are expressed as means ± SD. All experiments contained three to four replicates per experimental parameter.

Acknowledgments

We thank Andrew Assee for assistance with preliminary experiments, Dr. Diana M. Stafforini (University of Utah) and Dr. Takehiko Yokomizo (University of Tokyo) for advice, and Dr. Miriam Merad for critical reading of the manuscript. We also thank Dr. Thomas Dudler (ICOS Corporation) and Dr. Sem Saeland (Schering Plough) for provision of recombinant PAFAH and anti-langerin mAb, respectively. This work was supported by National Institutes of Health grants HL69446 and AI49653 to G.J.R. and HL61814 to E.A.F. Studies on *Pafr*$^{-/-}$ mice included support by grants-in-aid from the Minis-

try of Education, Science, Culture, Sports and Technology and the Ministry of Health, Labor, and Welfare of Japan (S.I. and T.S.). V.A. was supported by a postdoctoral fellowship from the European Molecular Biology Organization.

Received: April 20, 2004
Revised: September 10, 2004
Accepted: September 15, 2004
Published: October 19, 2004

References

Alderman, C.J., Bunyard, P.R., Chain, B.M., Foreman, J.C., Leake, D.S., and Katz, D.R. (2002). Effects of oxidised low density lipoprotein on dendritic cells: a possible immunoregulatory component of the atherogenic micro-environment? Cardiovasc. Res. *55*, 806–819.

Amara, A., Constans, J., Chaugier, C., Sebban, A., Dubourg, L., Peuchant, E., Pellegrin, J.L., Leng, B., Conri, C., and Geffard, M. (1995). Autoantibodies to malondialdehyde-modified epitope in connective tissue diseases and vasculitides. Clin. Exp. Immunol. *101*, 233–238.

Angeli, V., Faveeuw, C., Roye, O., Fontaine, J., Teissier, E., Capron, A., Wolowczuk, I., Capron, M., and Trottein, F. (2001). Role of parasite-derived prostaglandin D_2 in the inhibition of epidermal Langerhans cell migration during schistosomiasis infection. J. Exp. Med. *193*, 1135–1147.

Aprahamian, T., Rifkin, I., Bonegio, R., Hugel, B., Freyssinet, J.M., Sato, K., Castellot, J.J., Jr., and Walsh, K. (2004). Impaired clearance of apoptotic cells promotes synergy between atherogenesis and autoimmune disease. J. Exp. Med. *199*, 1121–1131.

Binder, C.J., Horkko, S., Dewan, A., Chang, M.K., Kieu, E.P., Goodyear, C.S., Shaw, P.X., Palinski, W., Witztum, J.L., and Silverman, G.J. (2003). Pneumococcal vaccination decreases atherosclerotic lesion formation: molecular mimicry between Streptococcus pneumoniae and oxidized LDL. Nat. Med. *9*, 736–743.

Bjorkbacka, H., Kunjathoor, V.V., Moore, K.J., Koehn, S., Ordija, C.M., Lee, M.A., Means, T., Halmen, K., Luster, A.D., Golenbock, D.T., and Freeman, M.W. (2004). Reduced atherosclerosis in MyD88-null mice links elevated serum cholesterol levels to activation of innate immunity signaling pathways. Nat. Med. *10*, 416–421.

Bobryshev, Y.V., Taksir, T., Lord, R.S., and Freeman, M.W. (2001). Evidence that dendritic cells infiltrate atherosclerotic lesions in apolipoprotein E-deficient mice. Histol. Histopathol. *16*, 801–808.

Breslow, J.L. (1996). Mouse models of atherosclerosis. Science *272*, 685–688.

Briles, D.E., Forman, C., Hudak, S., and Claflin, J.L. (1982). Anti-phosphorylcholine antibodies of the T15 idiotype are optimally protective against Streptococcus pneumoniae. J. Exp. Med. *156*, 1177–1185.

Burger, D., and Dayer, J.M. (2002). High-density lipoprotein-associated apolipoprotein A-I: the missing link between infection and chronic inflammation? Autoimmun. Rev. *1*, 111–117.

Cvetkovic, J.T., Wallberg-Jonsson, S., Ahmed, E., Rantapaa-Dahlqvist, S., and Lefvert, A.K. (2002). Increased levels of autoantibodies against copper-oxidized low density lipoprotein, malondialdehyde-modified low density lipoprotein and cardiolipin in patients with rheumatoid arthritis. Rheumatol. *41*, 988–995.

Dansky, H.M., Charlton, S.A., Barlow, C.B., Tamminen, M., Smith, J.D., Frank, J.S., and Breslow, J.L. (1999). Apo A-I inhibits foam cell formation in Apo E-deficient mice after monocyte adherence to endothelium. J. Clin. Invest. *104*, 31–39.

de Bont, N., Netea, M.G., Demacker, P.N., Verschueren, I., Kullberg, B.J., van Dijk, K.W., van der Meer, J.W., and Stalenhoef, A.F. (1999). Apolipoprotein E knock-out mice are highly susceptible to endotoxemia and Klebsiella pneumoniae infection. J. Lipid Res. *40*, 680–685.

Dentan, C., Tselepis, A.D., Chapman, M.J., and Ninio, E. (1996). Pefabloc, 4-[2-aminoethyl]benzenesulfonyl fluoride, is a new, potent nontoxic and irreversible inhibitor of PAF-degrading acetylhydrolase. Biochim. Biophys. Acta *1299*, 353–357.

Dichmann, S., Rheinen, H., Panther, E., Herouy, Y., Czech, W., Termeer, C., Simon, J.C., Gebicke-Haerter, P.J., and Norgauer, J. (2000). Downregulation of platelet-activating factor responsiveness during maturation of human dendritic cells. J. Cell. Physiol. *185*, 394–400.

Feingold, K.R., Elias, P.M., Mao-Qiang, M., Fartasch, M., Zhang, S.H., and Maeda, N. (1995). Apolipoprotein E deficiency leads to cutaneous foam cell formation in mice. J. Invest. Dermatol. *104*, 246–250.

Flores-Romo, L. (2001). In vivo maturation and migration of dendritic cells. Immunology *102*, 255–262.

Forte, T.M., Subbanagounder, G., Berliner, J.A., Blanche, P.J., Clermont, A.O., Jia, Z., Oda, M.N., Krauss, R.M., and Bielicki, J.K. (2002). Altered activities of anti-atherogenic enzymes LCAT, paraoxonase, and platelet-activating factor acetylhydrolase in atherosclerosis-susceptible mice. J. Lipid Res. *43*, 477–485.

Havel, R.J., Eder, H.A., and Bragdon, J.H. (1955). The distribution and chemical composition of ultracentrifugally separated lipoproteins in human serum. J. Clin. Invest. *34*, 1345–1353.

Hayem, G., Nicaise-Roland, P., Palazzo, E., de Bandt, M., Tubach, F., Weber, M., and Meyer, O. (2001). Anti-oxidized low-density-lipoprotein (OxLDL) antibodies in systemic lupus erythematosus with and without antiphospholipid syndrome. Lupus *10*, 346–351.

Heery, J.M., Kozak, M., Stafforini, D.M., Jones, D.A., Zimmerman, G.A., McIntyre, T.M., and Prescott, S.M. (1995). Oxidatively modified LDL contains phospholipids with platelet-activating factor-like activity and stimulates the growth of muscles cells. J. Clin. Invest. *96*, 2322–2330.

Ilowite, N.T., Samuel, P., Ginzler, E., and Jacobson, M.S. (1988). Dyslipoproteinemia in pediatric systemic lupus erythematosus. Arthritis Rheum. *31*, 859–863.

Ishii, S., and Shimizu, T. (2000). Platelet-activating factor (PAF) receptor and genetically engineered PAF receptor mutant mice. Prog. Lipid Res. *39*, 41–82.

Ishii, S., Kuwaki, T., Nagase, T., Maki, K., Tashiro, F., Sunaga, S., Cao, W.H., Kume, K., Fukuchi, Y., Ikuta, K., et al. (1998). Impaired anaphylactic responses with intact sensitivity to endotoxin in mice lacking a platelet-activating factor receptor. J. Exp. Med. *187*, 1779–1788.

Itano, A.A., McSorley, S.J., Reinhardt, R.L., Ehst, B.D., Ingulli, E., Rudensky, A.Y., and Jenkins, M.K. (2003). Distinct dendritic cell populations sequentially present antigen to CD4 T cells and stimulate different aspects of cell-mediated immunity. Immunity *19*, 47–57.

Laskowitz, D.T., Lee, D.M., Schmechel, D., and Staats, H.F. (2000). Altered immune responses in apolipoprotein E-deficient mice. J. Lipid Res. *41*, 613–620.

Libby, P. (2002). Inflammation in atherosclerosis. Nature *420*, 868–874.

Llodra, J., Angeli, V., Liu, J., Trogan, E., Fisher, E.A., and Randolph, G.J. (2004). Emigration of monocyte-derived cells from atherosclerotic lesions characterizes regressive, but not progressive, plaques. Proc. Natl. Acad. Sci. USA *101*, 11779–11784.

Ludewig, B., Jaggi, M., Dumrese, T., Brduscha-Riem, K., Odermatt, B., Hengartner, H., and Zinkernagel, R.M. (2001). Hypercholesterolemia exacerbates virus-induced immunopathologic liver disease via suppression of antiviral cytotoxic T cell responses. J. Immunol. *166*, 3369–3376.

Ludewig, B., Krebs, P., and Scandella, E. (2004). Immunopathogenesis of atherosclerosis. J. Leukoc. Biol. *76*, 300–306.

Marathe, G.K., Davies, S.S., Harrison, K.A., Silva, A.R., Murphy, R.C., Castro-Faria-Neto, H., Prescott, S.M., Zimmerman, G.A., and McIntyre, T.M. (1999). Inflammatory platelet-activating factor-like phospholipids in oxidized low density lipoproteins are fragmented alkyl phosphatidylcholines. J. Biol. Chem. *274*, 28395–28404.

Marathe, G.K., Zimmerman, G.A., and McIntyre, T.M. (2003). Platelet-activating factor acetylhydrolase, and not paraoxonase-1, is the oxidized phospholipid hydrolase of high density lipoprotein particles. J. Biol. Chem. *278*, 3937–3947.

McIntyre, T.M., Zimmerman, G.A., and Prescott, S.M. (1999). Biologi-

cally active oxidized phospholipids. J. Biol. Chem. *274*, 25189–25192.

McLachlan, J.B., Hart, J.P., Pizzo, S.V., Shelburne, C.P., Staats, H.F., Gunn, M.D., and Abraham, S.N. (2003). Mast cell-derived tumor necrosis factor induces hypertrophy of draining lymph nodes during infection. Nat. Immunol. *4*, 1199–1205.

Mehling, A., Loser, K., Varga, G., Metze, D., Luger, T.A., Schwarz, T., Grabbe, S., and Beissert, S. (2001). Overexpression of CD40 ligand in murine epidermis results in chronic skin inflammation and systemic autoimmunity. J. Exp. Med. *194*, 615–628.

Moazed, T.C., Kuo, C., Grayston, J.T., and Campbell, L.A. (1997). Murine models of Chlamydia pneumoniae infection and atherosclerosis. J. Infect. Dis. *175*, 883–890.

Montrucchio, G., Lupia, E., Battaglia, E., Del Sorbo, L., Boccellino, M., Biancone, L., Emanuelli, G., and Camussi, G. (2000). Platelet-activating factor enhances vascular endothelial growth factor-induced endothelial cell motility and neoangiogenesis in a murine matrigel model. Arterioscler. Thromb. Vasc. Biol. *20*, 80–88.

Netea, M.G., Demacker, P.N., de Bont, N., Boerman, O.C., Stalenhoef, A.F., van der Meer, J.W., and Kullberg, B.J. (1997). Hyperlipoproteinemia enhances susceptibility to acute disseminated Candida albicans infection in low-density-lipoprotein-receptor-deficient mice. Infect. Immun. *65*, 2663–2667.

O'Flaherty, J.T., Redman, J.F., Schmitt, J.D., Ellis, J.M., Surles, J.R., Marx, M.H., Piantadosi, C., and Wykle, R.L. (1987). 1-O-alkyl-2-N-methylcarbamyl-glycerophosphocholine: a biologically potent, non-metabolizable analog of platelet-activating factor. Biochem. Biophys. Res. Commun. *147*, 18–24.

Orekhov, A.N., Tertov, V.V., Kabakov, A.E., Adamova, I., Pokrovsky, S.N., and Smirnov, V.N. (1991). Autoantibodies against modified low density lipoprotein. Nonlipid factor of blood plasma that stimulates foam cell formation. Arterioscler. Thromb. *11*, 316–326.

Orem, A., Cimsit, G., Deger, O., Orem, C., and Vanizor, B. (1999). The significance of autoantibodies against oxidatively modified low-density lipoprotein (LDL) in patients with psoriasis. Clin. Chim. Acta *284*, 81–88.

Palframan, R.T., Jung, S., Cheng, G., Weninger, W., Luo, Y., Dorf, M., Littman, D.R., Rollins, B.J., Zweerink, H., Rot, A., and von Andrian, U.H. (2001). Inflammatory chemokine transport and presentation in HEV: a remote control mechanism for monocyte recruitment to lymph nodes in inflamed tissues. J. Exp. Med. *194*, 1361–1373.

Palinski, W., and Witztum, J.L. (2000). Immune responses to oxidative neoepitopes on LDL and phospholipids modulate the development of atherosclerosis. J. Intern. Med. *247*, 371–380.

Palinski, W., Ord, V.A., Plump, A.S., Breslow, J.L., Steinberg, D., and Witztum, J.L. (1994). ApoE-deficient mice are a model of lipoprotein oxidation in atherogenesis. Demonstration of oxidation-specific epitopes in lesions and high titers of autoantibodies to malondialdehyde-lysine in serum. Arterioscler. Thromb. *14*, 605–616.

Palinski, W., Miller, E., and Witztum, J.L. (1995). Immunization of low density lipoprotein (LDL) receptor-deficient rabbits with homologous malondialdehyde-modified reduces atherogenesis. Proc. Natl. Acad. Sci. USA *92*, 821–825.

Plump, A.S., Scott, C.J., and Breslow, J.L. (1994). Human apolipoprotein A-I gene expression increases high density lipoprotein and suppresses atherosclerosis in the apolipoprotein E-deficient mouse. Proc. Natl. Acad. Sci. USA *91*, 9607–9611.

Quarck, R., De Geest, B., Stengel, D., Mertens, A., Lox, M., Theilmeier, G., Michiels, C., Raes, M., Bult, H., Collen, D., et al. (2001). Adenovirus-mediated gene transfer of human platelet-activating factor-acetylhydrolase prevents injury-induced neointima formation and reduces spontaneous atherosclerosis in apolipoprotein E-deficient mice. Circulation *103*, 2495–2500.

Randolph, G.J., Beaulieu, S., Lebecque, S., Steinman, R.M., and Muller, W.A. (1998a). Differentiation of monocytes into dendritic cells in a model of transendothelial trafficking. Science *282*, 480–483.

Randolph, G.J., Beaulieu, S., Pope, M., Sugawara, I., Hoffman, L., Steinman, R.M., and Muller, W.A. (1998b). A physiologic function for p-glycoprotein (MDR-1) during the migration of dendritic cells from skin via afferent lymphatic vessels. Proc. Natl. Acad. Sci. USA *95*, 6924–6929.

Robbiani, D.F., Finch, R.A., Jager, D., Muller, W.A., Sartorelli, A.C., and Randolph, G.J. (2000). The leukotriene C(4) transporter MRP1 regulates CCL19 (MIP-3beta, ELC)-dependent mobilization of dendritic cells to lymph nodes. Cell *103*, 757–768.

Rong, J.X., and Fisher, E.A. (2000). High-density lipoprotein: gene-based approaches to the prevention of atherosclerosis. Ann. Med. *32*, 642–651.

Rong, J.X., Li, J., Reis, E.D., Choudhury, R.P., Dansky, H.M., Elmalem, V.I., Fallon, J.T., Breslow, J.L., and Fisher, E.A. (2001). Elevating high-density lipoprotein cholesterol in apolipoprotein E-deficient mice remodels advanced atherosclerotic lesions by decreasing macrophages and increasing smooth muscle cell content. Circulation *104*, 2447–2452.

Roselaar, S.E., and Daugherty, A. (1998). Apolipoprotein E-deficient mice have impaired innate immune responses to Listeria monocytogenes in vivo. J. Lipid Res. *39*, 1740–1743.

Ross, R. (1993). The pathogenesis of atherosclerosis: a perspective for the 1990s. Nature *362*, 801–809.

Schuler, G., and Steinman, R.M. (1985). Murine epidermal Langerhans cells mature into potent immunostimulatory dendritic cells in vitro. J. Exp. Med. *161*, 526–546.

Schultz, J.R., Verstuyft, J.G., Gong, E.L., Nichols, A.V., and Rubin, E.M. (1993). Protein composition determines the anti-atherogenic properties of HDL in transgenic mice. Nature *365*, 762–764.

Sekigawa, I., Nawata, M., Seta, N., Yamada, M., Iida, N., and Hashimoto, H. (2002). Cytomegalovirus infection in patients with systemic lupus erythematosus. Clin. Exp. Rheumatol. *20*, 559–564.

Shimaoka, T., Nakayama, T., Hieshima, K., Kume, N., Fukumoto, N., Minami, M., Hayashida, K., Kita, T., Yoshie, O., and Yonehara, S. (2004). Chemokines generally exhibit scavenger receptor activity through their receptor-binding domain. J. Biol. Chem. *279*, 26807–26810.

Sozzani, S., Longoni, D., Bonecchi, R., Luini, W., Bersani, L., D'Amico, G., Borsatti, A., Bussolino, F., Allavena, P., and Mantovani, A. (1997). Human monocyte-derived and CD34+ cell-derived dendritic cells express functional receptors for platelet activating factor. FEBS Lett. *418*, 98–100.

Stafforini, D.M., Satoh, K., Atkinson, D.L., Tjoelker, L.W., Eberhardt, C., Yoshida, H., Imaizumi, T., Takamatsu, S., Zimmerman, G.A., McIntyre, T.M., et al. (1996). Platelet-activating factor acetylhydrolase deficiency. A missense mutation near the active site of an anti-inflammatory phospholipase. J. Clin. Invest. *97*, 2689–2690.

Tjoelker, L.W., and Stafforini, D.M. (2000). Platelet-activating factor acetylhydrolases in health and disease. Biochim. Biophys. Acta *1488*, 102–123.

Tselepis, A.D., Elisaf, M., Besis, S., Karabina, S.A., Chapman, M.J., and Siamopoulou, A. (1999). Association of the inflammatory state in active juvenile rheumatoid arthritis with hypo-high-density lipoproteinemia and reduced lipoprotein-associated platelet-activating factor acetylhydrolase activity. Arthritis Rheum. *42*, 373–383.

Van Lenten, B.J., Wagner, A.C., Anantharamaiah, G.M., Garber, D.W., Fishbein, M.C., Adhikary, L., Nayak, D.P., Hama, S., Navab, M., and Fogelman, A.M. (2002). Influenza infection promotes macrophage traffic into arteries of mice that is prevented by D-4F, an apolipoprotein A-I mimetic peptide. Circulation *106*, 1127–1132.

van Ree, J.H., Gijbels, M.J., van den Broek, W.J., Hofker, M.H., and Havekes, L.M. (1995). Atypical xanthomatosis in apolipoprotein E-deficient mice after cholesterol feeding. Atherosclerosis *112*, 237–243.

Wick, G., Knoflach, M., and Xu, Q. (2004). Autoimmune and inflammatory mechanisms in atherosclerosis. Annu. Rev. Immunol. *22*, 361–403.

Witmer-Pack, M.D., Hughes, D.A., Schuler, G., Lawson, L., McWilliam, A., Inaba, K., Steinman, R.M., and Gordon, S. (1993). Identification of macrophages and dendritic cells in the osteopetrotic (op/op) mouse. J. Cell Sci. *104*, 1021–1029.

Wu, R., Svenungsson, E., Gunnarsson, I., Andersson, B., Lundberg, I., Schafer Elinder, L., and Frostegard, J. (1999). Antibodies against lysophosphatidylcholine and oxidized LDL in patients with SLE. Lupus *8*, 142–150.

Yamada, Y., Ichihara, S., Fujimura, T., and Yokota, M. (1998). Identification of the G994→ T missense in exon 9 of the plasma platelet-activating factor acetylhydrolase gene as an independent risk factor for coronary artery disease in Japanese men. Metabolism *47*, 177–181.

Zebrack, J.S., and Anderson, J.L. (2003). The role of infection in the pathogenesis of cardiovascular disease. Prog. Cardiovasc. Nurs. *18*, 42–49.